

drug resistance profile but also for tracking the global epidemiology of clinically important organisms.

Acknowledgment

We thank Naemah Logan for her expertise and guidance.

About The Author

Dr. Caldera is a clinical microbiology fellow at the University of California, Los Angeles, California. His primary research interest focuses on the development of diagnostic assays that use advanced molecular and sequencing techniques in clinical microbiology.

References

1. National Institutes of Health, National Institute of Allergy and Infectious Diseases. *Shigellosis* [cited 2023 Mar 23]. <https://www.niaid.nih.gov/diseases-conditions/shigellosis>
2. Centers for Disease Control and Prevention. Shigella infection among gay, bisexual, and other men who have sex with men [cited 2023 Mar 24]. <https://www.cdc.gov/shigella/msm.html>
3. Charles H, Prochazka M, Thorley K, Crewdson A, Greig DR, Jenkins C, et al.; Outbreak Control Team. Outbreak of sexually transmitted, extensively drug-resistant *Shigella sonnei* in the UK, 2021–22: a descriptive epidemiological study. *Lancet Infect Dis.* 2022;22:1503–10. [https://doi.org/10.1016/S1473-3099\(22\)00370-X](https://doi.org/10.1016/S1473-3099(22)00370-X)
4. Thorley K, Charles H, Greig DR, Prochazka M, Mason LCE, Baker KS, et al. Emergence of extensively drug-resistant and multidrug-resistant *Shigella flexneri* serotype 2a associated with sexual transmission among gay, bisexual, and other men who have sex with men, in England: a descriptive epidemiological study. *Lancet Infect Dis.* 2023;S1473-3099 (22)00807-6. [https://doi.org/10.1016/S1473-3099\(22\)00807-6](https://doi.org/10.1016/S1473-3099(22)00807-6)
5. Lefèvre S, Njamkepo E, Feldman S, Ruckly C, Carle I, Lejay-Collin M, et al. Rapid emergence of extensively drug-resistant *Shigella sonnei* in France. *Nat Commun.* 2023;14:462. <https://doi.org/10.1038/s41467-023-36222-8>
6. Hasman H, Saputra D, Sicheritz-Ponten T, Lund O, Svendsen CA, Frimodt-Møller N, et al. Rapid whole-genome sequencing for detection and characterization of microorganisms directly from clinical samples. *J Clin Microbiol.* 2014;52:139–46. <https://doi.org/10.1128/JCM.02452-13>
7. Larsen MV, Cosentino S, Lukjancenko O, Saputra D, Rasmussen S, Hasman H, et al. Benchmarking of methods for genomic taxonomy. *J Clin Microbiol.* 2014;52:1529–39. <https://doi.org/10.1128/JCM.02981-13>
8. Clausen PTL, Aarestrup FM, Lund O. Rapid and precise alignment of raw reads against redundant databases with KMA. *BMC Bioinformatics.* 2018;19:307. <https://doi.org/10.1186/s12859-018-2336-6>
9. Kamau E, Adamson PC, Crandall J, Mukhopadhyay R, Yang S. Discovery of a novel sub-lineage of multi-drug resistant *Shigella flexneri* in southern California. *Int J Infect Dis.* 2023;132:1–3. <https://doi.org/10.1016/j.ijid.2023.03.039>

Address for correspondence: Daniel Z. Uslan, UCLA Division of Infectious Diseases, David Geffen School of Medicine at UCLA, Ste 301, 911 Broxton Ave, Los Angeles, CA 90024, USA; email: duslan@mednet.ucla.edu

Novel Highly Pathogenic Avian Influenza A(H5N1) Clade 2.3.4.4b Virus in Wild Birds, South Korea

Sun-hak Lee, Andrew Y. Cho, Tae-hyeon Kim, Seo-jeong Ahn, Ju Ho Song, Heesu Lee, Yun-Jeong Choi, Nyamsuren Otgontogtokh, Jung-Hoon Kwon, Chang-Seon Song, Dong-Hun Lee

Author affiliations: Konkuk University, Seoul, South Korea (S.-h. Lee, A.Y. Cho, T.-h. Kim, S.-j. Ahn, J.H. Song, H. Lee, Y.-J. Choi, N. Otgontogtokh, C.-S. Song, D.-H. Lee); Kyungpook National University, Daegu, South Korea (J.-H. Kwon)

DOI: <https://doi.org/10.3201/eid2907.221893>

We isolated 5 highly pathogenic avian influenza A(H5N1) clade 2.3.4.4.b viruses from wild waterfowl feces in South Korea during November 2022. Whole-genome sequencing and phylogenetic analysis revealed novel genotypes produced by reassortment with Eurasian low pathogenicity avian influenza viruses. Enhanced surveillance will be required to improve prevention and control strategies.

Highly pathogenic avian influenza viruses (HPAIVs) have caused major economic losses in the poultry industry and are a major threat to public health. Since the first detection of HPAIV A(H5N1) from a goose in 1996 in Guangdong, China, its descendants have evolved into multiple hemagglutinin (HA) gene-specific clades (H0–H9) and subclades (1) causing intercontinental epizootics (2). Over several decades, H5 HPAIVs have evolved into multiple subtypes and genotypes generated by reassortment with low pathogenicity avian influenza viruses (LPAIVs), which led to emergence of clade 2.3.4.4 H5Nx HPAIVs in eastern China during 2013–2014 (3).

In mid-2016, reassortant H5N8 clade 2.3.4.4b HPAIVs that contained internal genes of LPAIVs from Eurasia were detected in wild birds at Uvs-Nuur Lake in Russia and Qinghai Lake in China (4); the viruses caused large outbreaks in Europe during 2016–2017 (5). Subsequently, various novel reassortant H5N8 HPAIVs were detected in Eurasia (5,6). In late 2020, novel reassortant clade 2.3.4.4b H5N1 HPAIVs were detected and became predominant in Europe in poultry and wild birds (5).

We isolated 5 H5N1 HPAIVs from wild bird feces collected in South Korea in November 2022 (Appendix 1, <https://wwwnc.cdc.gov/EID/>

Table 1. Nucleotide sequence identities between gene segments of 5 novel clade 2.3.4.4b highly pathogenic avian influenza A(H5N1) viruses from wild birds in South Korea and nearest homologs in the GISAID Epiflu database*

| Isolates | Gene | Virus | Accession no.† | % Identity | |
|----------------|---|---|--|------------|--------|
| All 5 isolates | PB2 | A/goose/Hunan/SE284/2022(H5N1)/HPAI | EPI2029895 | 99.21% | |
| | | A/duck/Mongolia/826/2019 (H4N6)/LP AI | EPI1777578 | 98.33% | |
| | HA | A/turkey/Tyumen/81-96V/2021 (H5N1)/HPAI | EPI1958105 | 99.47% | |
| | | A/chicken/Tyumen/47-79V/2021 (H5N1)/HPAI | EPI1957985 | 99.41% | |
| | NA | A/goose/Hunan/SE284/2022 (H5N1)/HPAI | EPI2029897 | 99.22% | |
| | | A/duck/Bangladesh/51600/2021 (H5N1)/HPAI | EPI2163444 | 99.15% | |
| | M | A/ibis/Egypt/RLQP-229S/2022 (H5N1)/HPAI | EPI2201158 | 99.80% | |
| | | A/duck/Bangladesh/19D1817/2021 (H5N1)/HPAI | EPI2062119 | 99.80% | |
| | K22-730-1, K22-742, K22-856-2, K22-862-1‡ | PB1 | A/Mallard/South Korea/KNU2019-20/2019 (H5N1)/LP AI | EPI1902594 | 98.77% |
| | | | A/duck/Saga/411117/2013 (H6N1)/LP AI | EPI855573 | 98.72% |
| PA | | A/duck/Bangladesh/18D1811/2022 (H5N3)/LP AI | EPI1997269 | 99.44% | |
| | | A/duck/Bangladesh/17D1839/2022 (H5N3)/LP AI | EPI1997245 | 99.44% | |
| NP | | A/Northern Shoveler/South Korea/KNU2021-13/2021 (H11N9)/LP AI | EPI2153438 | 99.40% | |
| NS | | A/Mallard/South Korea/KNU2019-51/2019 (H5N3)/LP AI | EPI1902887 | 99.33% | |
| | | A/mallard/Yakutia/47/2020 (H7N7)/LP AI | EPI1848197 | 99.52% | |
| K22-920§ | PB1 | A/Wild duck/South Korea/KNU2020-31/2020 (H1N1)/LP AI | EPI1931606 | 99.40% | |
| | | A/mallard/Anhui/3-617/2019 (H6N1)/LP AI | EPI1743666 | 98.46% | |
| | PA | A/Eurasian_Curlew/China/CZ322(7)/2019 (H3N8)/LP AI | EPI1890551 | 98.46% | |
| | | A/common teal/Amur region/92b/2020 (H6N2)/LP AI | EPI1849993 | 99.26% | |
| | NP | A/mallard/Russia Primorje/94T/2020 (H1N1)/LP AI | EPI1849961 | 99.21% | |
| | | A/Spot-billed duck/South Korea/KNU2020-105/2020 (H3N2)/LP AI | EPI1931651 | 99.33% | |
| | NS | A/Eurasian teal/South Korea/JB32-15/2019 (H10N7)/LP AI | EPI1903752 | 98.80% | |
| | | A/mallard/Yakutia/47/2020 (H7N7)/LP AI | EPI1848197 | 99.28% | |
| | | | A/duck/Bangladesh/39397/2019 (H10N3)/LP AI | EPI1778261 | 99.28% |

*HPAI influenza viruses isolated from wild bird feces in November 2022. HA, hemagglutinin; HPAI, highly pathogenic avian influenza; LP AI, low pathogenicity avian influenza; M, matrix protein; NP, nucleoprotein; NS, nonstructural; PA, polymerase acidic; PB, polymerase basic.

†Accession numbers of nearest homologs as of December 8, 2022, from GISAID (<https://www.gisaid.org>).

‡Genotype I.

§Genotype II.

article/29/7/22-1893-App1.pdf): A/Spot-billed_duck/Korea/K22-730-1/2022(H5N1) [K22-730-1], A/Wild_bird/Korea/K22-742/2022(H5N1) [K22-742], A/Spot-billed_duck/Korea/K22-856-2/2022(H5N1) [K22-856-2], A/Spot-billed_duck/Korea/K22-862-1/2022(H5N1) [K22-862-1], and A/Spot-billed_duck/Korea/K22-920/2022(H5N1) [K22-920] (Appendix 1 Table 1). To rapidly share the information, we conducted whole-genome sequencing of the isolates and deposited the genome sequences in the GISAID database (<https://www.gisaid.org>).

All H5N1 isolates were classified as HPAIV on the basis of HA cleavage site amino acid sequences (PLRPKRRKR/G). The 5 isolates shared high nucleotide sequence identities (99.4% to ~100%) across all 8 influenza genes, except for the K22-920 isolate polymerase basic protein 1 (PB1), polymerase acidic protein (PA), nucleoprotein (NP), and nonstructural (NS) genes (93.0% to ~99.0%). BLAST (<https://blast.ncbi.nlm.nih.gov>) search results showed HA, neuraminidase, and matrix (M) protein genes of all isolates had >99.1% identities with 2021–2022 clade 2.3.4.4b HPAIVs (Table 1). PB1, PA, NP, and NS genes of all isolates were highly similar (98.72%–99.52%) to 2019–2022 LP AIVs from East Asia. PB1, PA, NP, and NS genes of K22-920 were similar to 2019–2020 LP AIVs from South Korea, Russia, and Bangladesh (>98.4%–99.3%).

In maximum-likelihood phylogenetic analyses, PB2, HA, neuraminidase, and M genes of the 5 H5N1 viruses from South Korea clustered with those of viruses previously described as genotype G10, identified in China during 2022–2023 (Appendix 1 Figures 1–8); G10 is a natural reassortant H5N1 HPAIV containing the PB2 gene from LP AIVs (7). PB1, PA, NP, and NS genes of all H5N1 viruses from South Korea except K22-920 clustered with those of LP AIVs from Asia; those gene segments in K22-920 clustered separately with other LP AIVs from Asia, including South Korea, Russia, and Bangladesh (Appendix 1 Figures 2, 3, 5, 8). Bayesian phylogeny of the HA gene indicated the H5N1 viruses from South Korea formed a well-supported cluster; time to most recent common ancestor was estimated to be August 11, 2022 (95% highest posterior density June 11–October 11, 2022), suggesting those H5N1 HPAIVs most likely emerged 1–2 months before the autumn wild bird migration to South Korea (Figure 1; Appendix 1 Figure 9). The isolates from South Korea shared recent common ancestry with the A/Jiangsu/NJ210/2023(H5N1) virus; time to most recent common ancestor between them was April 12, 2022 (95% highest posterior density December 26, 2021–July 28, 2022), suggesting the ancestral H5N1 HPAIVs had been circulating undetected for ~7 months.

The H5N1 HPAIVs from South Korea contained amino acids in HA with binding affinity for avian α -2,3-linked sialic acid receptors (T118, V210, Q222, and G224) (H5 numbering) (8,9). They also had 2 HA amino acid substitutions, S113A and T156A, associated with increased binding affinity to human α -2,6-

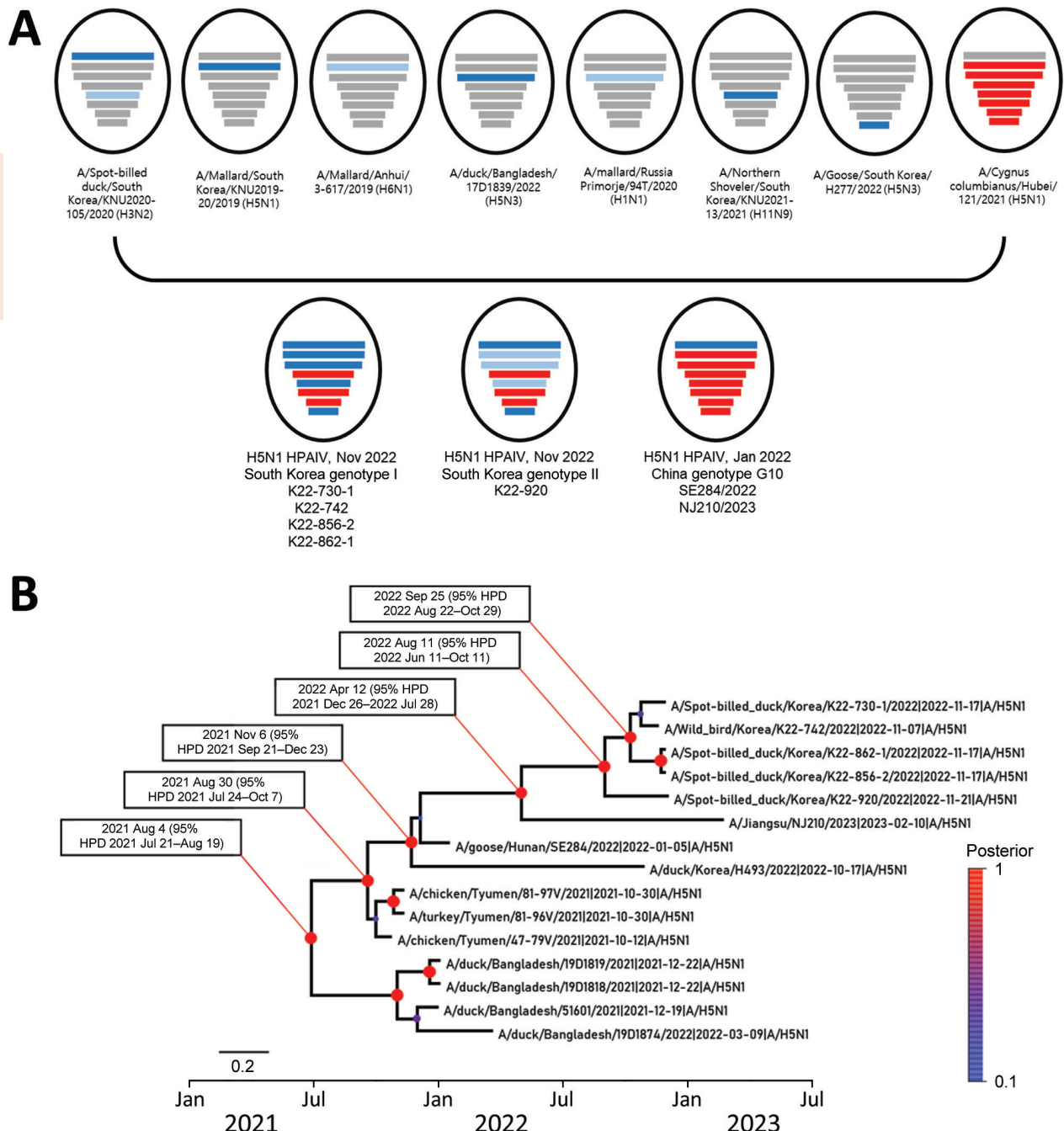


Figure 1. Phylogenetic analysis of novel highly pathogenic avian influenza A(H5N1) clade 2.3.4.4b viruses found in wild bird feces in South Korea, November 2022. A) Schematic representation of origin of virus isolates from South Korea compared with genotype G10 viruses found in China. Bars represent 8 gene segments of avian influenza virus in the following order (top to bottom): polymerase basic 2, polymerase basic 1, polymerase acidic, hemagglutinin, nucleoprotein, neuraminidase, matrix, and nonstructural. Different bar colors indicate different virus origins estimated from maximum-likelihood phylogenetic trees. Gene segments originating from highly pathogenic avian influenza viruses are indicated by red bars. Gene segments originating from low pathogenicity avian influenza viruses are indicated by blue bars. B) Time-scaled maximum clade credibility tree for hemagglutinin gene segments from novel viruses isolated in South Korea (5 viruses at top). Red to blue colored scale on right side indicates posterior clade probabilities at nodes. Scale bar indicates nucleotide substitutions per site. HPD, highest posterior density.

linked sialic acid receptors (Appendix 1 Table 2). All 5 isolates had amino acid substitutions that included A515T in PA, known to increase polymerase activity in mammal cells, and N30D, I43M, T215A in MP1 and L89V in PB2, known to increase virulence in mice (Appendix 1 Tables 2, 3).

The HPAI/LPAI reassortment of H5Nx clade 2.3.4.4b HPAIVs created a diverse genetic pool of H5 clade 2.3.4.4 viruses that continuously emerged in various countries (1). Clade 2.3.4.4 H5N8 HPAIV isolated from Uvs-Nuur Lake in Russia had reassorted H3N8 LPAIV genes from Mongolia (4). In Europe, HPAIVs identified in 2020 (5,6) were produced by reassortment between clade 2.3.4.4b HPAIV and LPAIVs from Eurasia. Novel reassortments of clade 2.3.4.4 HPAIV and LPAIVs from Eurasia were also detected in 2016 (10), during 2020–2021 (Appendix 1 reference 1), and in late 2021 (Appendix 1 reference 2) in South Korea. Considering the continuous emergence and global dissemination of novel reassortant clade 2.3.4.4b HPAI H5Nx viruses, enhanced active surveillance in wild animals and domestic poultry will be required to monitor the introduction, dissemination, and evolution of HPAIVs and provide insight for improved prevention and control strategies.

Acknowledgments

We thank our colleagues worldwide for their laboratory contributions, which are made available through GISAID (Appendix 2, <https://wwwnc.cdc.gov/EID/article/29/7/22-1893-App2.xlsx>).

This research was supported by the Bio and Medical Technology Development Program of the National Research Foundation, funded by the government of South Korea (grant no. NRF-2018M3A9H405635).

About the Author

Mr. Lee is a PhD candidate at Konkuk University, Seoul, South Korea. His primary research interests focus on molecular epidemiology and host–pathogen interactions of avian influenza viruses.

References

- Gu M, Liu W, Cao Y, Peng D, Wang X, Wan H, et al. Novel reassortant highly pathogenic avian influenza (H5N5) viruses in domestic ducks, China. *Emerg Infect Dis*. 2011;17:1060–3. <https://doi.org/10.3201/eid1706.101406>
- Lee DH, Criado MF, Swayne DE. Pathobiological origins and evolutionary history of highly pathogenic avian influenza viruses. *Cold Spring Harb Perspect Med*. 2021;11:a038679. <https://doi.org/10.1101/cshperspect.a038679>
- Lee Y-J, Kang H-M, Lee E-K, Song B-M, Jeong J, Kwon Y-K, et al. Novel reassortant influenza A(H5N8) viruses, South Korea, 2014. *Emerg Infect Dis*. 2014;20:1087–9. <https://doi.org/10.3201/eid2006.140233>
- Lee DH, Sharshov K, Swayne DE, Kurskaya O, Sobolev I, Kabilov M, et al. Novel reassortant clade 2.3.4.4 avian influenza A(H5N8) virus in wild aquatic birds, Russia, 2016. *Emerg Infect Dis*. 2017;23:359–60. <https://doi.org/10.3201/eid2302.161252>
- Pohlmann A, King J, Fusaro A, Zecchin B, Banyard AC, Brown IH, et al. Has epizootic become enzootic? Evidence for a fundamental change in the infection dynamics of highly pathogenic avian influenza in Europe, 2021. *mBio*. 2022;13:e0060922. <https://doi.org/10.1128/mbio.00609-22>
- Lewis NS, Banyard AC, Whittard E, Karibayev T, Al Kafagi T, Chvala I, et al. Emergence and spread of novel H5N8, H5N5 and H5N1 clade 2.3.4.4 highly pathogenic avian influenza in 2020. *Emerg Microbes Infect*. 2021;10:148–51. <https://doi.org/10.1080/22221751.2021.1872355>
- Cui P, Shi J, Wang C, Zhang Y, Xing X, Kong H, et al. Global dissemination of H5N1 influenza viruses bearing the clade 2.3.4.4b HA gene and biologic analysis of the ones detected in China. *Emerg Microbes Infect*. 2022;11:1693–704. <https://doi.org/10.1080/22221751.2022.2088407>
- Burke DF, Smith DJ. A recommended numbering scheme for influenza A HA subtypes. *PLoS One*. 2014;9:e112302. <https://doi.org/10.1371/journal.pone.0112302>
- Suttie A, Deng YM, Greenhill AR, Dussart P, Horwood PF, Karlsson EA. Inventory of molecular markers affecting biological characteristics of avian influenza A viruses. *Virus Genes*. 2019;55:739–68. <https://doi.org/10.1007/s11262-019-01700-z>
- Kwon JH, Lee DH, Swayne DE, Noh JY, Yuk SS, Erdene-Ochir TO, et al. Reassortant clade 2.3.4.4 avian influenza A(H5N6) virus in a wild mandarin duck, South Korea, 2016. *Emerg Infect Dis*. 2017;23:822–6. <https://doi.org/10.3201/eid2305.161905>

Address for correspondence: Dong-Hun Lee, Wildlife Health Laboratory, College of Veterinary Medicine, Konkuk University, Seoul, South Korea; email: donghunlee@konkuk.ac.kr

Novel Highly Pathogenic Avian Influenza A(H5N1) Clade 2.3.4.4b Virus in Wild Birds, South Korea

Appendix 1

Additional Methods

Virus Detection and Isolation

A total of 3,490 wild waterfowl fecal samples were collected during September 8–November 23, 2022. Only fresh fecal samples in wild bird habitats, including Gokgyo stream, Anseong stream, and Miho River in South Korea, were collected for routine highly pathogenic avian influenza A virus (HPAIV) surveillance. Those sites were selected because numerous avian influenza viruses have been identified previously, including H5Nx HPAIVs (3). The fecal samples were resuspended in phosphate-buffered saline containing 400 mg/mL gentamycin and then clarified by centrifugation (3,000 rpm for 10 min at 4°C). Supernatants were filtered through a 0.45 µm syringe filter and used to inoculate 10-day-old specific pathogen-free embryonated chicken eggs for virus isolation. Harvested allantoic fluids were tested for hemagglutinin (HA) activity. Total RNA was extracted from allantoic fluids positive for HA by using the RNeasy mini kit (QIAGEN, <https://www.qiagen.com>) according to the manufacturer's instructions. RNA was tested for H5 and H7 subtypes and influenza A virus matrix protein gene by real-time reverse transcription PCR as previously described (4). Influenza A–positive and H5–positive samples were detected in 3 of 30 collection trips (Appendix 1 Table 1). Host species for the viruses were identified by DNA barcoding the cytochrome c oxidase subunit 1 gene as previously described (5).

Whole-Genome Sequencing and Assembly

All 8 virus genes from each isolate were amplified by using the OneTaq 2× Master Mix (New England BioLabs, <https://www.neb.com>) and universal primers as previously described

(6). Next generation sequencing was performed on an iSeq100 instrument (Illumina, <https://www.illumina.com>). Library preparation was performed by using the Illumina DNA library prep kit. Whole genome sequences were assembled by using the Iterative Refinement Meta-Assembler (<https://wonder.cdc.gov/amd/flu/irma>) module and an in-house shell script. Assembly was visualized by using Geneious Prime software (<https://www.geneious.com>). Assembled genomes were uploaded in the GISAID EpiFlu database (<https://www.gisaid.org>) under accession nos. EPI_15943002, EPI_15943015, EPI_15944663, EPI_15944665, EPI_15944667) (Appendix 1 Table 1)

Phylogenetic Inference

We conducted BLAST (<https://blast.ncbi.nlm.nih.gov>) searches in the GISAID EpiFlu database and retrieved the top 100 hits for comparative phylogenetic analysis. We also used genome sequences of representative HPAI viruses that have been identified in Asia, Europe, and North America since 2021. Complete coding regions were aligned by using MAFFT (<https://mafft.cbrc.jp/alignment/software>). We generated maximum-likelihood trees of each gene segment by using the RAxML program and general time-reversible plus gamma nucleotide substitution model with 1,000 rapid bootstrap replicates (7) (Appendix 1 Figures 1–8). We performed Bayesian relaxed-clock phylogenetic analysis of HA genes by using BEAST version 1.10.4 (<https://beast.community>) and applied an uncorrelated log-normal distribution relaxed-clock method; the Hasegawa, Kishino, and Yano plus gamma nucleotide substitution model; and Gaussian Markov random field Bayesian Skyride coalescent prior method (Appendix 1 Figure 9). A Markov chain Monte Carlo method (8) to sample trees and evolutionary parameters was run for 50–100 million generations. Independent chains (≥ 3) were combined for adequate sampling of the posterior distribution of the trees. The output data were analyzed by using TRACER v1.4 (<https://beast.bio.ed.ac.uk/tracer>) with 5% burn-in. A maximum clade credibility tree was generated by using TreeAnnotator in BEAST and visualized with FigTree v1.4.2 (<https://tree.bio.ed.ac.uk>).

References

1. Baek YG, Lee YN, Lee DH, Shin JI, Lee JH, Chung DH, et al. Multiple reassortants of H5N8 clade 2.3.4.4b highly pathogenic avian influenza viruses detected in South Korea during the winter of 2020–2021. *Viruses*. 2021;13:490. [PubMed https://doi.org/10.3390/v13030490](https://doi.org/10.3390/v13030490)

2. Sagong M, Lee YN, Song S, Cha RM, Lee EK, Kang YM, et al. Emergence of clade 2.3.4.4b novel reassortant H5N1 high pathogenicity avian influenza virus in South Korea during late 2021. *Transbound Emerg Dis.* 2022;69:e3255–60. [PubMed](#) <https://doi.org/10.1111/tbed.14551>
3. Cui P, Shi J, Wang C, Zhang Y, Xing X, Kong H, et al. Global dissemination of H5N1 influenza viruses bearing the clade 2.3.4.4b HA gene and biologic analysis of the ones detected in China. *Emerg Microbes Infect.* 2022;11:1693–704. [PubMed](#) <https://doi.org/10.1080/22221751.2022.2088407>
4. Spackman E, Senne DA, Bulaga LL, Myers TJ, Perdue ML, Garber LP, et al. Development of real-time RT-PCR for the detection of avian influenza virus. *Avian Dis.* 2003;47:1079–82. [PubMed](#) <https://doi.org/10.1637/0005-2086-47.s3.1079>
5. Lee DH, Lee HJ, Lee YJ, Kang HM, Jeong OM, Kim MC, et al. DNA barcoding techniques for avian influenza virus surveillance in migratory bird habitats. *J Wildl Dis.* 2010;46:649–54. [PubMed](#) <https://doi.org/10.7589/0090-3558-46.2.649>
6. Lee DH. Complete genome sequencing of influenza A viruses using next-generation sequencing. *Methods Mol Biol.* 2020;2123:69–79. [PubMed](#) https://doi.org/10.1007/978-1-0716-0346-8_6
7. Stamatakis A. RAxML version 8: a tool for phylogenetic analysis and post-analysis of large phylogenies. *Bioinformatics.* 2014;30:1312–3. [PubMed](#) <https://doi.org/10.1093/bioinformatics/btu033>
8. Suchard MA, Weiss RE, Sinsheimer JS. Bayesian selection of continuous-time Markov chain evolutionary models. *Mol Biol Evol.* 2001;18:1001–13. [PubMed](#) <https://doi.org/10.1093/oxfordjournals.molbev.a003872>

Appendix 1 Table 1. Clade 2.3.4.4b H5N1 highly pathogenic avian influenza viruses isolated in this study.

| Identification | Subtype | Collection Date | Host species* | Collection location | Latitude | Longitude | GISAIID no. |
|---|---------|-----------------|---------------------|----------------------------|----------|-----------|--------------|
| A/Spot-billed_duck/Korea/K22-730-1/2022 | H5N1 | 2022 Nov 17 | Anas poecilorhyncha | Asan-si, Gokgyo stream | 36.79785 | 127.0072 | EPI_15943002 |
| A/Wild_bird/Korea/K22-742/2022 | H5N1 | 2022 Nov 07 | NI | Asan-si, Gokgyo stream | 36.79785 | 127.0072 | EPI_15943015 |
| A/Spot-billed_duck/Korea/K22-856-2/2022 | H5N1 | 2022 Nov 17 | Anas poecilorhyncha | Anseong-si, Anseong stream | 36.99126 | 127.2079 | EPI_15944663 |
| A/Spot-billed_duck/Korea/K22-862-1/2022 | H5N1 | 2022 Nov 17 | Anas poecilorhyncha | Anseong-si, Anseong stream | 36.99126 | 127.2079 | EPI_15944665 |
| A/Spot-billed_duck/Korea/K22-920/2022 | H5N1 | 2022 Nov 21 | Anas poecilorhyncha | Cheongju-si, Miho River | 36.65164 | 127.3781 | EPI_15944667 |

*Host species were identified by DNA Barcoding of mitochondrial DNA. NI, not identified.

Appendix 1 Table 2. Amino acid substitutions in hemagglutinin and polymerase basic 2 proteins from clade 2.3.4.4b H5N1 highly pathogenic avian influenza viruses isolated in South Korea, November 2022*

| Isolate | Hemagglutinin† | | | | | | | | | | Polymerase basic protein 2‡ | | | | |
|-------------|----------------|-------|-----|-------|-------|-------|-------|-------|-------|-------|-----------------------------|-------|-------|-------|-------|
| | D94N | S123A | 126 | S133A | S154N | T156A | T188I | V210I | Q222L | G224S | L89V | D256G | Q591K | E627K | D701N |
| Genotype I | S | P | E | A | D | A | T | V | Q | G | V | D | Q | E | D |
| Genotype II | S | P | E | A | D | A | T | V | Q | G | V | D | Q | E | D |
| Hunan/SE284 | S | P | E | A | D | A | T | V | Q | G | V | D | Q | E | D |

*Genotype I contained isolates K22-730-1, K22-742, K22-856-2, and K22-862-1 from South Korea. Genotype II contained isolate K22-920 from South Korea. Hunan/SE284 was genotype G10 isolated from China.

†Hemagglutinin H5 subtype numbering was used. D94N, S123P, S133A, S154N, T156A, T188I, Q222L, and G224S mutations in hemagglutinin are associated with increased binding to human α -2,6 sialic acid receptors.

‡L89V and D256G mutations in PB2 are known to be associated with increased virulence in mice. Q591K, E627K, and D701N mutations in PB2 are associated with increased viral replication in mammals.

Appendix 1 Table 3 Amino acid substitutions in polymerase acidic, matrix, and nonstructural proteins from clade 2.3.4.4b H5N1 highly pathogenic avian influenza viruses isolated in South Korea, November 2022*

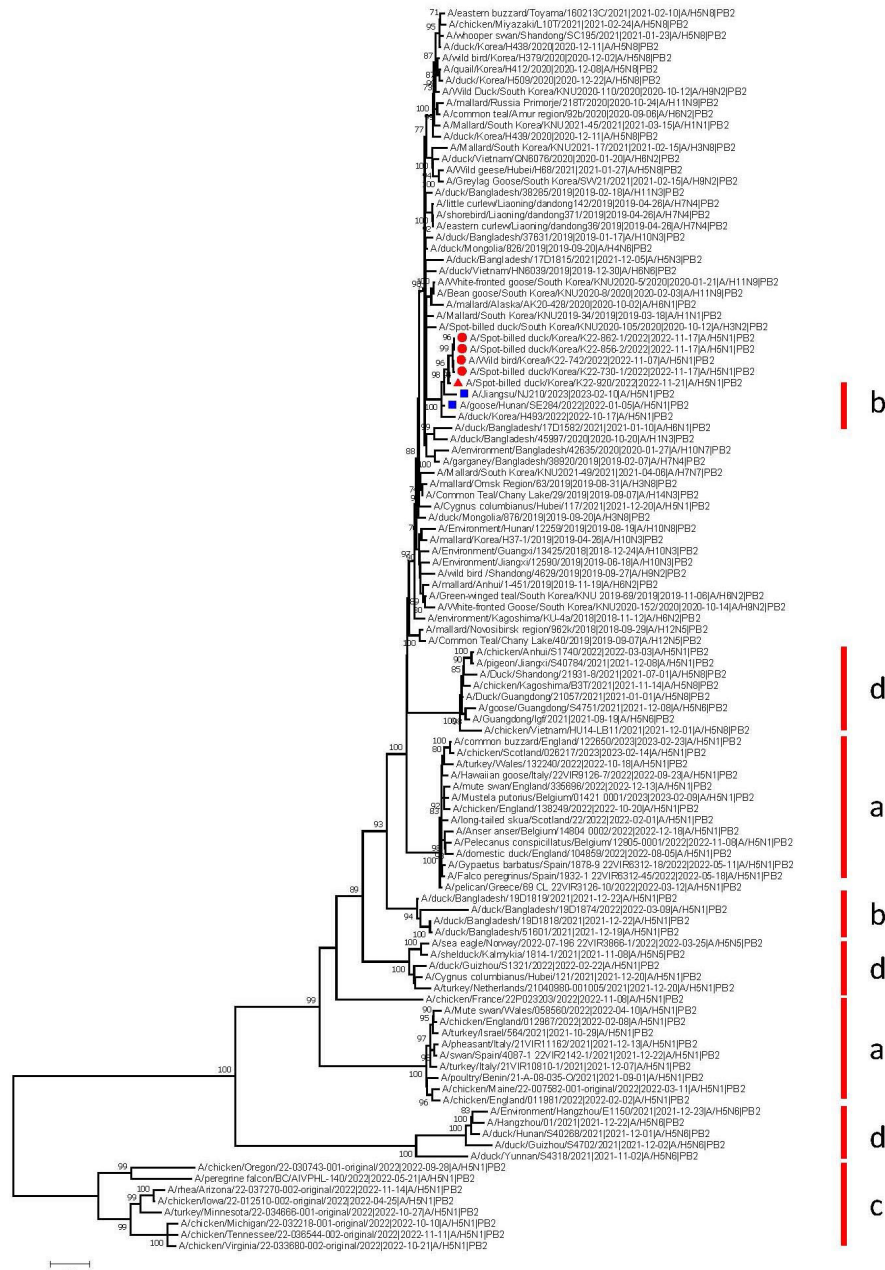
| Isolate | PA† | Matrix protein 1‡ | | | | Nonstructural protein§ | | | | |
|-------------|-------|-------------------|------|-------|------|------------------------|------|-------|------|--|
| | A515T | N30D | I43M | T215A | P42S | Δ 80-84 | L98F | I101M | ESEV | |
| Genotype I | T | D | M | A | A | AIASS | I | E | ESEV | |
| Genotype II | T | D | M | A | A | AIASS | I | E | ESEV | |
| Hunan/SE284 | T | D | M | A | S | TIAPV | M | D | ESEV | |

*Genotype I contained isolates K22-730-1, K22-742, K22-856-2, and K22-862-1 from South Korea. Genotype II contained isolate K22-920 from South Korea. Hunan/SE284 was genotype G10 isolated from China. PA, polymerase acidic protein.

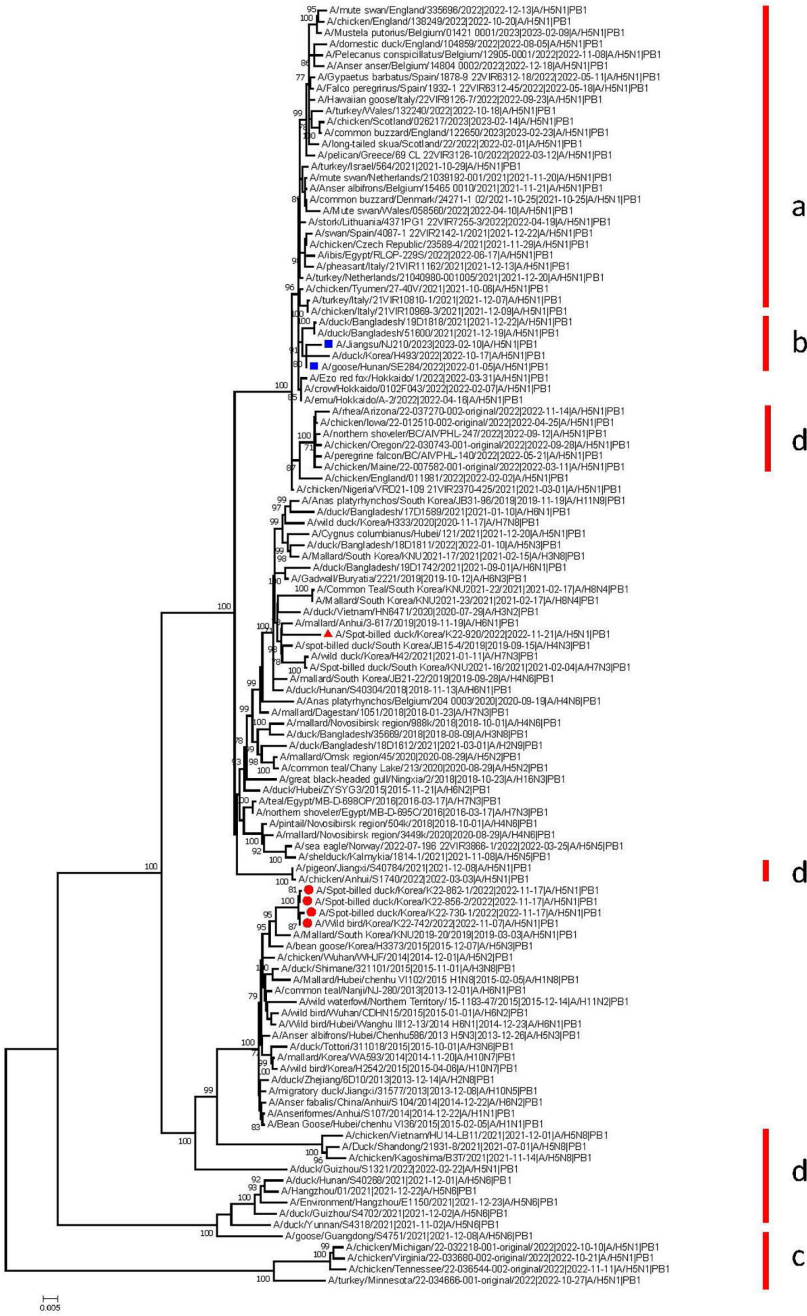
†A515T mutation in PA is known to be associated with avian influenza subtype H5 transmissibility in ferrets.

‡N30D, I43M, and T215A mutations in matrix protein 1 are known to be associated with increased virulence in mice.

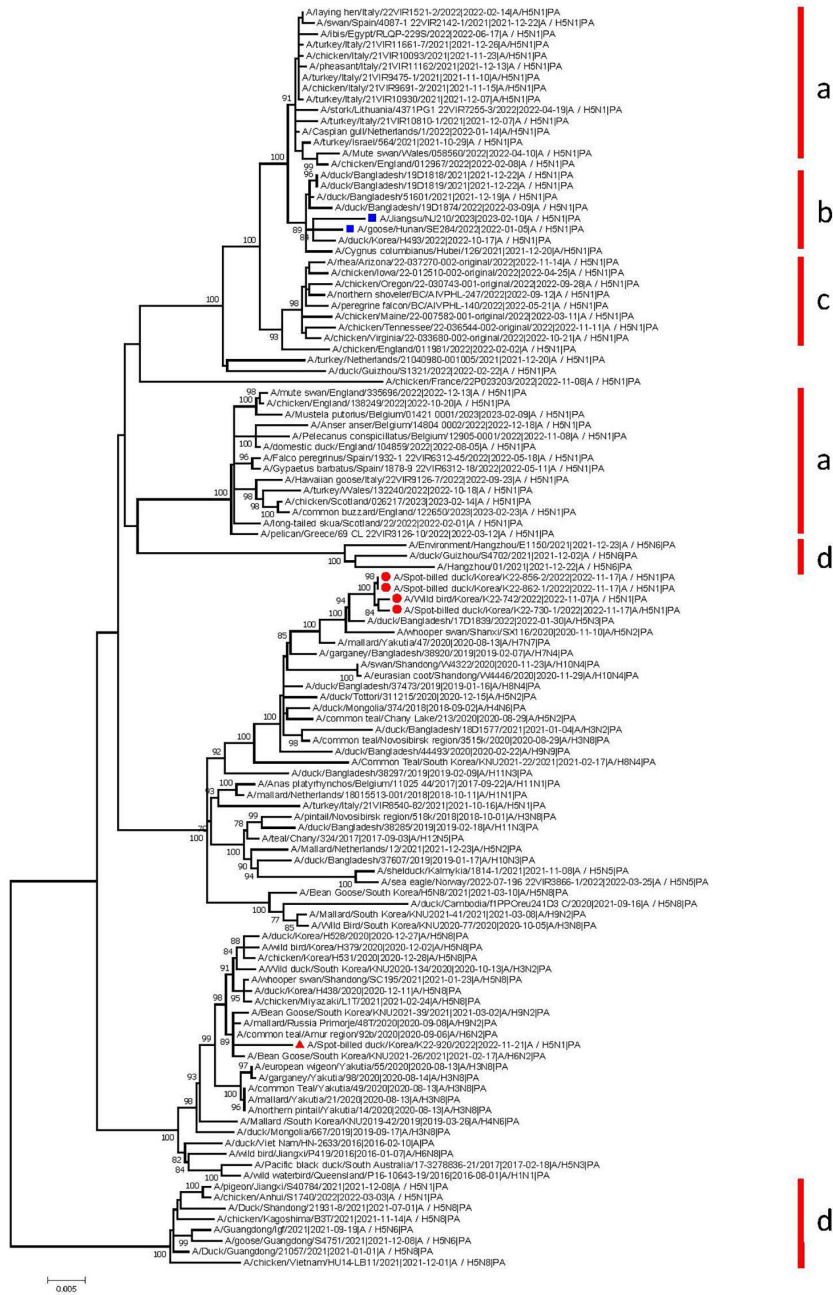
§P42S mutation, 80-84 deletion, and ESEV PDZ-binding motif mutations in nonstructural protein are known to be associated with increased virulence in mice.



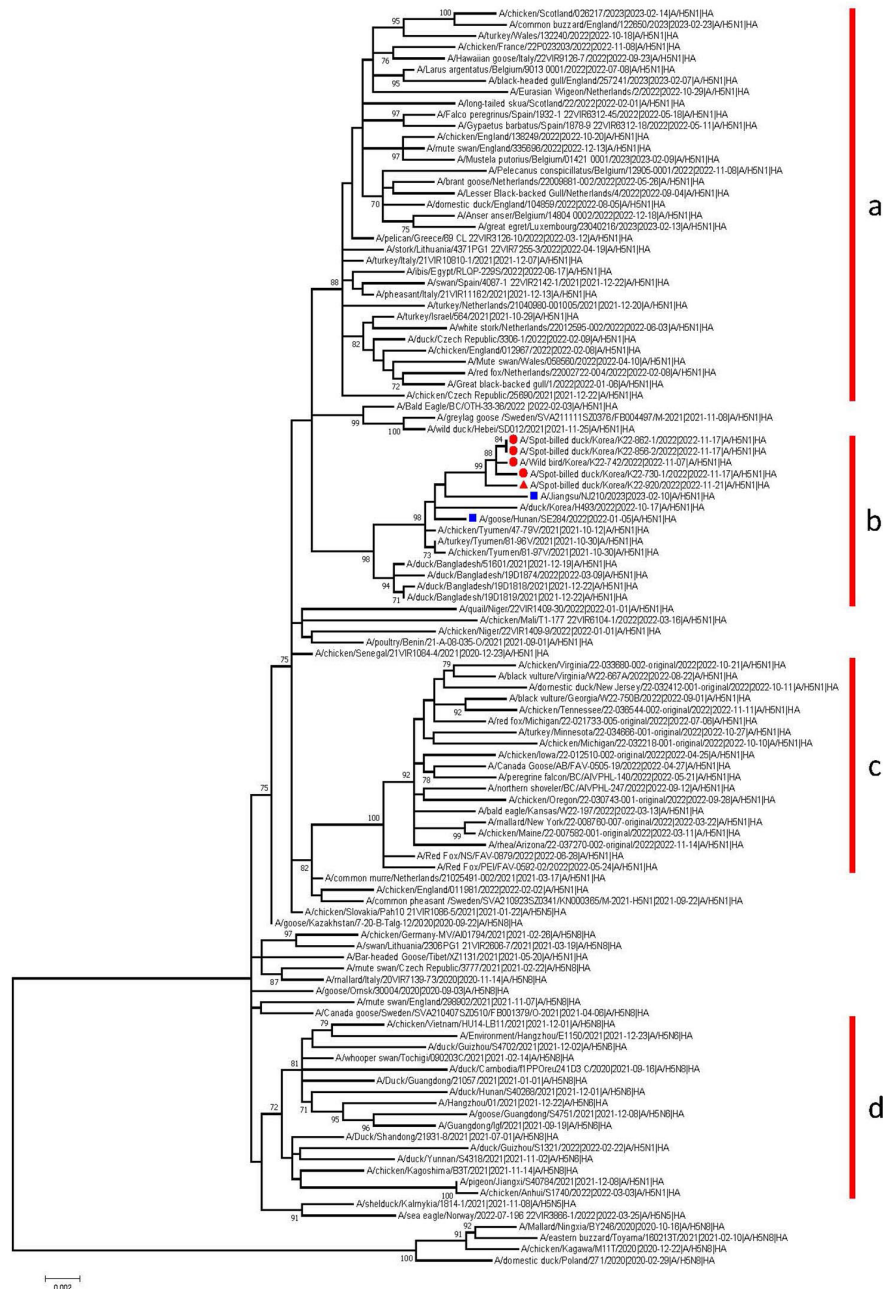
Appendix 1 Figure 1. Maximum-likelihood phylogenetic tree of polymerase basic 2 gene segment from avian influenza viruses. Bootstrap values >70% are shown. Highly pathogenic avian influenza virus isolates K22–862–1, K22–856–2, K22–742, K22–730–1 from South Korea are indicated by solid red circles, K22–920 from South Korea by solid red triangle, and genotype G10 isolates A/Hunan/SE284/2022 and A/Jiangsu/NJ10/2023 from China by blue rectangles. Red vertical lines indicate gene clusters mainly detected in Europe (a), Asia, including Bangladesh, Russia, and China (b), North America (c), and East Asia, including Japan, China, Vietnam, and Cambodia (d). Scale bar indicates nucleotide substitutions per site.



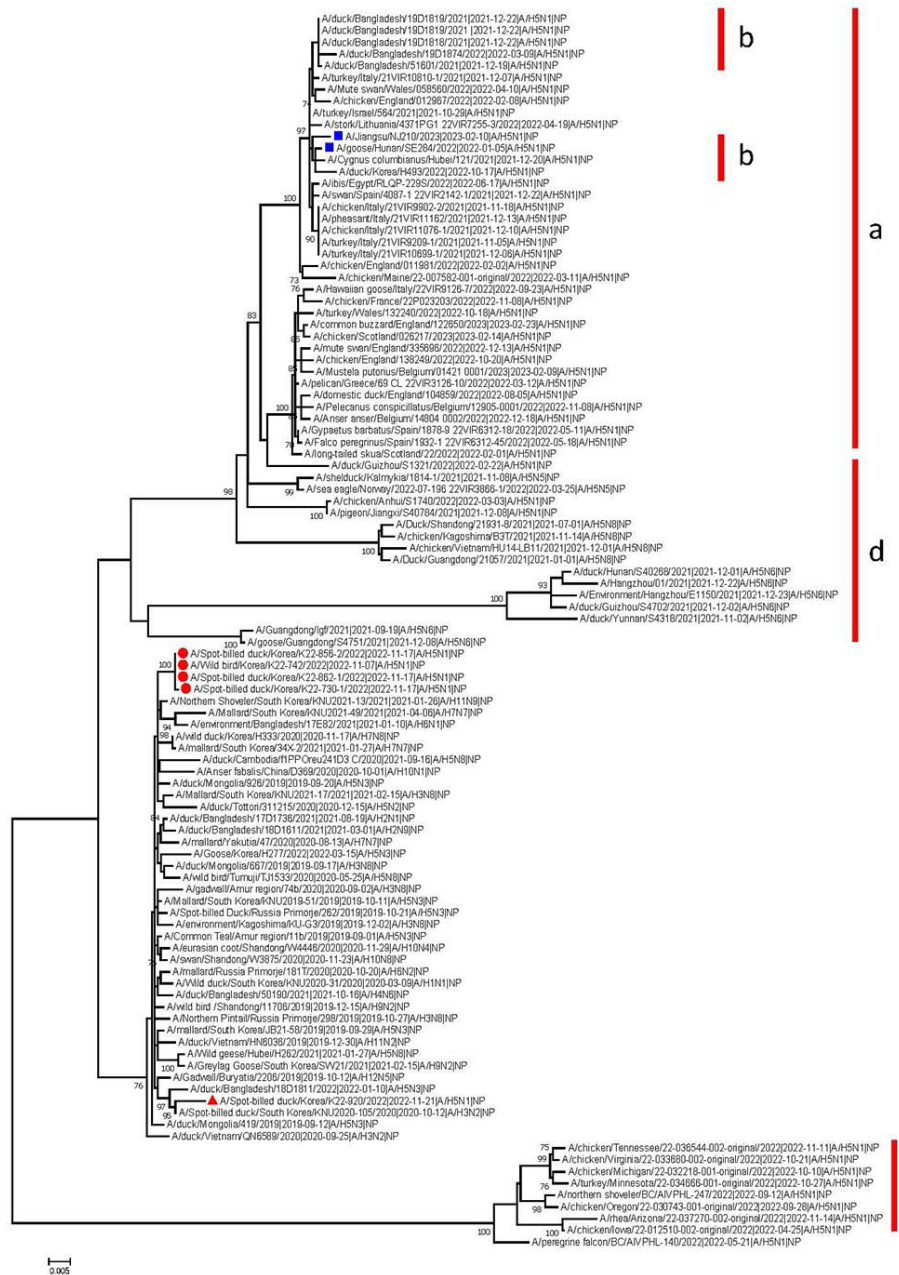
Appendix 1 Figure 2. Maximum-likelihood phylogenetic tree of polymerase basic 1 protein gene segment from avian influenza viruses. Bootstrap values >70% are shown. Highly pathogenic avian influenza virus isolates K22–862–1, K22–856–2, K22-742, K22–730–1 from South Korea are indicated by solid red circles, K22–920 from South Korea by solid red triangle, and genotype G10 isolates A/Hunan/SE284/2022 and A/Jiangsu/NJ10/2023 from China by blue rectangles. Red vertical lines indicate gene clusters mainly detected in Europe (a), Asia, including Bangladesh, Russia, and China (b), North America (c), and East Asia, including Japan, China, Vietnam, and Cambodia (d). Scale bar indicates nucleotide substitutions per site.



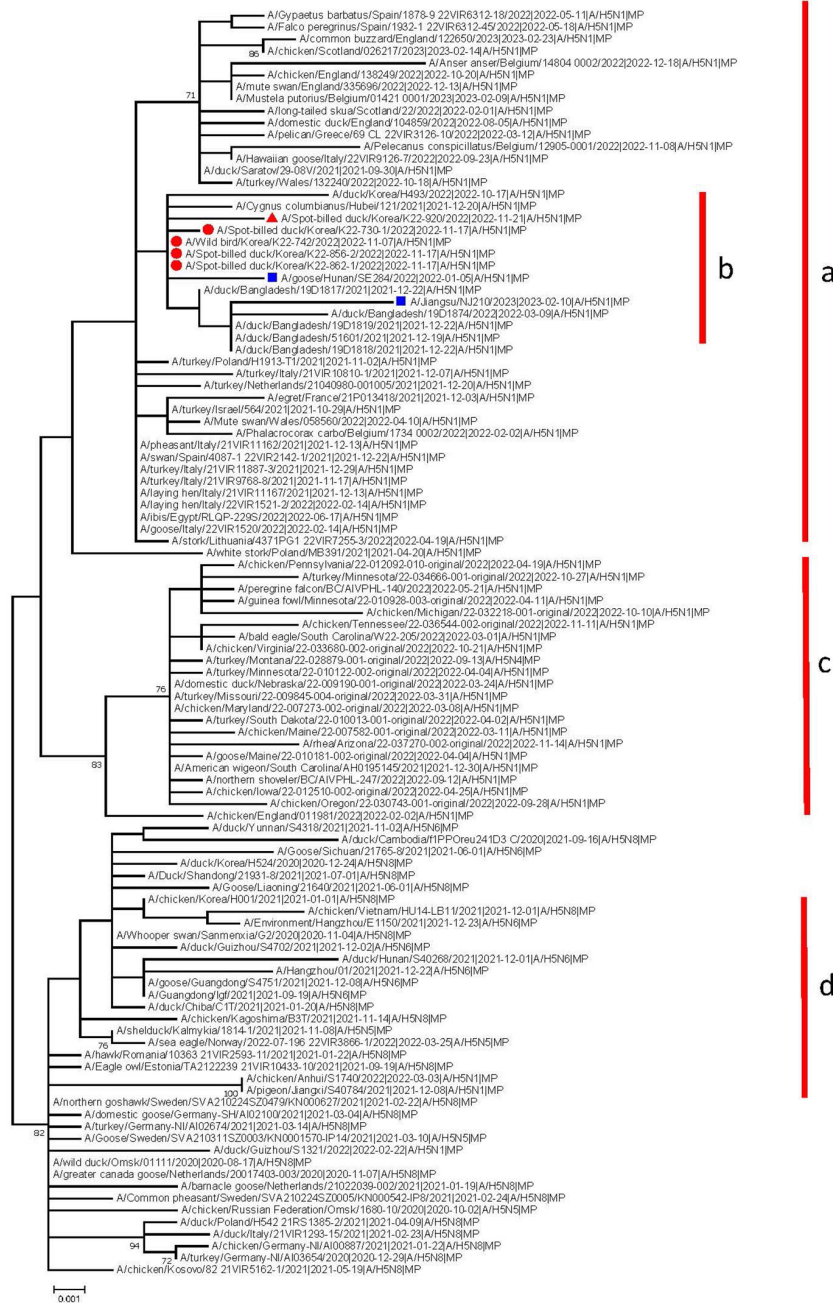
Appendix 1 Figure 3. Maximum-likelihood phylogenetic tree of polymerase acidic protein gene segment from avian influenza viruses. Bootstrap values >70% are shown. Highly pathogenic avian influenza virus isolates K22–862–1, K22–856–2, K22–742, K22–730–1 from South Korea are indicated by solid red circles, K22–920 from South Korea by solid red triangle, and genotype G10 isolates A/Hunan/SE284/2022 and A/Jiangsu/NJ10/2023 from China by blue rectangles. Red vertical lines indicate gene clusters mainly detected in Europe (a), Asia, including Bangladesh, Russia, and China (b), North America (c), and East Asia, including Japan, China, Vietnam, and Cambodia (d). Scale bar indicates nucleotide substitutions per site.



Appendix 1 Figure 4. Maximum-likelihood phylogenetic tree of hemagglutinin gene segment from avian influenza viruses. Bootstrap values >70% are shown. Highly pathogenic avian influenza virus isolates K22–862–1, K22–856–2, K22–742, K22–730–1 from South Korea are indicated by solid red circles, K22–920 from South Korea by solid red triangle, and genotype G10 isolates A/Hunan/SE284/2022 and A/Jiangsu/NJ10/2023 from China by blue rectangles. Red vertical lines indicate gene clusters mainly detected in Europe (a), Asia, including Bangladesh, Russia, and China (b), North America (c), and East Asia, including Japan, China, Vietnam, and Cambodia (d). Scale bar indicates nucleotide substitutions per site.



Appendix 1 Figure 5. Maximum-likelihood phylogenetic tree of nucleoprotein gene segment from avian influenza viruses. Bootstrap values >70% are shown. Highly pathogenic avian influenza virus isolates K22–862–1, K22–856–2, K22–742, K22–730–1 from South Korea are indicated by solid red circles, K22–920 from South Korea by solid red triangle, and genotype G10 isolates A/Hunan/SE284/2022 and A/Jiangsu/NJ10/2023 from China by blue rectangles. Red vertical lines indicate gene clusters mainly detected in Europe (a), Asia, including Bangladesh, Russia, and China (b), North America (c), and East Asia, including Japan, China, Vietnam, and Cambodia (d). Scale bar indicates nucleotide substitutions per site.



Appendix 1 Figure 6. Maximum-likelihood phylogenetic tree of neuraminidase gene segment of avian influenza viruses. Bootstrap values >70% are shown. Highly pathogenic avian influenza virus isolates K22–862–1, K22–856–2, K22–742, K22–730–1 from South Korea are indicated by solid red circles, K22–920 from South Korea by solid red triangle, and genotype G10 isolates A/Hunan/SE284/2022 and A/Jiangsu/NJ10/2023 from China by blue squares. Red vertical lines indicate gene clusters mainly detected in Europe (a), Asia, including Bangladesh, Russia, and China (b), North America (c), and East Asia, including Japan, China, Vietnam, and Cambodia (d). Scale bar indicates nucleotide substitutions per site.



Appendix 1 Figure 7. Maximum-likelihood phylogenetic tree of matrix protein gene segment from avian influenza viruses. Bootstrap values >70% are shown. Highly pathogenic avian influenza virus isolates K22–862–1, K22–856–2, K22–742, K22–730–1 from South Korea are indicated by solid red circles, K22–920 from South Korea by solid red triangle, and genotype G10 isolates A/Hunan/SE284/2022 and A/Jiangsu/NJ10/2023 from China by blue rectangles. Red vertical lines indicate gene clusters mainly detected in Europe (a), Asia, including Bangladesh, Russia, and China (b), North America (c), and East Asia, including Japan, China, Vietnam, and Cambodia (d). Scale bar indicates nucleotide substitutions per site.



Appendix 1 Figure 8. Maximum-likelihood phylogenetic tree of nonstructural protein gene segment from avian influenza viruses. Bootstrap values >70% are shown. Highly pathogenic avian influenza virus isolates K22–862–1, K22–856–2, K22–742, K22–730–1 from South Korea are indicated by solid red circles, K22–920 from South Korea by solid red triangle, and genotype G10 isolates A/Hunan/SE284/2022 and A/Jiangsu/NJ10/2023 from China by blue rectangles. Red vertical lines indicate gene clusters mainly detected in Europe (a), Asia, including Bangladesh, Russia, and China (b), North America (c), and East Asia, including Japan, China, Vietnam, and Cambodia (d). Scale bar indicates nucleotide substitutions per site.



Appendix 1 Figure 9. Time-scaled maximum clade credibility phylogenetic tree of hemagglutinin gene segments of avian influenza viruses. Node bars represent 95% Bayesian credible intervals. The x-axis defines the time scale in decimal years. Highly pathogenic avian influenza virus isolates K22–862–1, K22–856–2, K22–742, K22–730–1 from South Korea are indicated by solid red circles, K22–920 from South Korea is indicated by solid red triangle, and genotype G10 isolates A/Hunan/SE284/2022 and A/Jiangsu/NJ10/2023 from are indicated by blue rectangles. Scale bar indicates nucleotide substitutions per site.